

# PREPARATION OF Fe/GLASS COMPOSITE BY REDUCTION OF $\text{Na}_2\text{O}-\text{Fe}_2\text{O}_3-\text{B}_2\text{O}_3-\text{SiO}_2-\text{ZnO}$ GLASS AND GLASS CERAMICS

A. Mohammadpour, S. M. Mirkazemi and A. Beitollahi

\* [mirkazemi@iust.ac.ir](mailto:mirkazemi@iust.ac.ir)

Received: January 2015

Accepted: June 2015

School of Metallurgy and Materials Engineering, Iran University of Science and Technology, Tehran, Iran.

**Abstract:** In the present study, the feasibility of  $\alpha$ -Fe ferromagnetic phase formation in glass and glass-ceramic by reduction in hydrogen atmosphere have been investigated. The glass with the composition of  $35\text{Na}_2\text{O}-24\text{Fe}_2\text{O}_3-20\text{B}_2\text{O}_3-20\text{SiO}_2-1\text{ZnO}$  (mol %) was melted and quenched by using a twin roller technique. As quenched glass flakes were heat treated in the range of  $400-675^\circ\text{C}$  for 1-2 h in hydrogen atmosphere, which resulted in reduction of iron cations to  $\alpha$ -Fe and FeO. The reduction of iron cations in glass was not completely occurred. Saturation magnetization of these samples was  $8-37\text{ emu g}^{-1}$ . For the formation of glass ceramic, As quenched glass flakes heat treated at  $590^\circ\text{C}$  for 1 h. Heat treatment of glass ceramic containing magnetite at  $675^\circ\text{C}$  in hydrogen atmosphere for 1 h led to reduction of almost all of the iron cations to  $\alpha$ -Fe. Saturation magnetization of this sample increased from  $19.8\text{ emu g}^{-1}$  for glass ceramic to  $67\text{ emu g}^{-1}$ .

**Keywords:** Magnetite,  $\alpha$ -Fe, Reduction, Glass, Glass Ceramic, Magnetic Composite

## 1. INTRODUCTION

Soft magnetic composites (SMCs) are ferromagnetic particles coated with a thin electrically insulating layer and then pressed into the desired shape by the powder metallurgy (PM) methods. SMCs have unique magnetic properties, such as a three-dimensional (3D) isotropic ferromagnetic behavior, low eddy current loss, relatively lower total core loss at medium and high frequencies, and flexible design, which can be applied to various fields [1–5]. To provide the maximum magnetic permeability, the amount of inter-particle insulation should be minimized and the iron content maximized. Several researchers have tried to improve the magnetic performance of SMCs by selecting suitable insulating materials and applying various coating methods [6, 7]. Currently, insulating coatings include epoxy, polyamide, silicon resins and poly-vinyl alcohol [8–10]. The thermal treatment temperature for these materials is limited by the thermal resistance of the organic insulating layer between the magnetic particles; therefore phosphates (zinc/iron/manganese) and oxides ( $\text{MgO}$ ,  $\text{SiO}_2$ ) with high resistance temperatures were selected instead of organic coatings [11-12]. Various

methods have been explored to synthesize metal/insulator nanocomposites, including sol-gel [13], sputtering [14], electrodeposition [15], high energy ball milling [16], microemulsion and reverse micelle techniques [17]. Most of these methods are complex and expensive with low yield. In the present study, a new kind of SMC with glass matrix was obtained by a simple method which was reduction of glass and glass ceramic containing Fe cations. This novel method could be used to produce SMCs with different compositions and magnetic properties with low cost.

## 2. EXPERIMENTAL

### 2.1. Glass Formation

The nominal chemical compositions of prepared glasses was  $35\text{Na}_2\text{O}-24\text{Fe}_2\text{O}_3-20\text{B}_2\text{O}_3-20\text{SiO}_2-1\text{ZnO}$  (mol %). The raw materials were reagent grade  $\text{Na}_2\text{CO}_3$ ,  $\text{CaCO}_3$ ,  $\text{Fe}_2\text{O}_3$ ,  $\text{ZnO}$ ,  $\text{SiO}_2$  and  $\text{B}(\text{OH})_3$ . The batches were melted in alumina crucibles in  $1300-1350^\circ\text{C}$  range, with a holding time of 15 min at the final temperature. The melts were then quenched between rotating steel rollers.

## 2. 2. Glass-Ceramics Formation

For crystallization of glass, resulting flakes ~50  $\mu\text{m}$  thick were heat treated under a graphite powder bed. According to previous research [18] time and temperature of heat treatment was selected 1 h and 590  $^{\circ}\text{C}$  respectively.

## 2. 3. Reduction of Glass and Glass Ceramics

Flakes of glass and powder of glass ceramic (<53  $\mu\text{m}$ ) samples were introduced in a silica tube placed in a furnace. They were heated under argon flow until the desired treatment temperature was reached. Then argon was replaced by hydrogen (450-500 ml/min) at atmospheric pressure. Treatment times were between 1 and 2 h, and temperature in the range 400 to 675  $^{\circ}\text{C}$ . At the end of this time, hydrogen was replaced by argon and the furnace was allowed to cool to room temperature by switching off the power. One of the glass samples was maintained in 590  $^{\circ}\text{C}$  for 2 h in Ar atmosphere before reduction. The synthesis condition of samples is shown in table 1.

## 2. 4. Characterization

The phase identification of the samples were studied by X-ray diffraction (XRD) (PANalytical X'Pert Pro MPD) using Cu K $\alpha$  radiation. The magnetization measurements were carried out by vibrating sample magnetometer (VSM) MDK6 Meghnatis daghigh kavir, mizan daghigh.

**Table 1.** Heat treatment conditions of samples.

Sample	Crystallization		Reduction in H <sub>2</sub> atmosphere	
	Temp. ( $^{\circ}\text{C}$ )	Time (h)	Temp. ( $^{\circ}\text{C}$ )	Time (h)
GC	590	1	-	-
GR-400-2	-	-	400	2
CR-590-1	-	-	590	1
GR-657-2	-	-	675	2
GR-590-2-675-1	590	2	675	2
GCR-675-1	590	1	675	1

## 3. RESULT AND DISCUSSION

### 3. 1. Glass and Glass Ceramic

XRD patterns of the glass (Fig. 1) illustrates that the sample is amorphous in the accuracy range of XRD analysis.

Fig. 2 depicts the XRD pattern of glass ceramic. It reveals the existence of  $\alpha\text{-Na}_2\text{Si}_2\text{O}_5$  and  $\alpha\text{-Na}_2\text{B}_6\text{O}_{10}$  phases besides magnetite in this sample. Using Scherrer's equation the mean particle size of magnetite phase in this sample was calculated as 21 nm. Also The X-ray diffraction pattern of the sample contains the peaks of iron silicate phases. By consuming Fe cations, the formation of these phases leads to a decrease in the amount of magnetite phase in final glass ceramic.

Hysteresis loop of glass and glass ceramic is shown in fig. 3 and 4 respectively. Maximum magnetization of the glass was 1.6 emu g<sup>-1</sup> and the saturation wasn't observed in the curve. The value of the magnetization is probably due to the formation of magnetite phase during cooling of the glass melt and it is not detectable by XRD analysis because the amount of crystalline phase was negligible. The reason that curve has not been reached to the saturation could be the possible existence of superparamagnetic particles in glass [18].

The saturation magnetization (Ms) of the glass

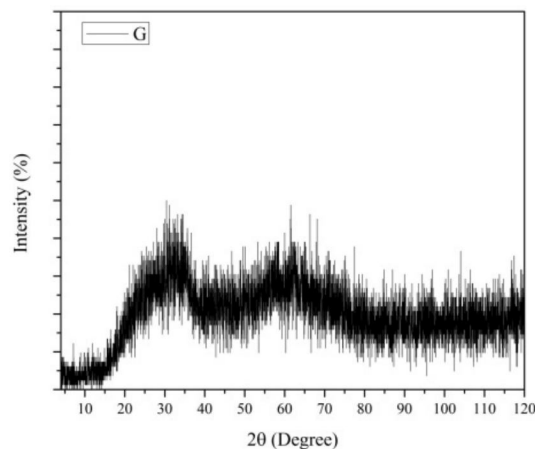


**Fig. 1.** XRD pattern of glass (G).

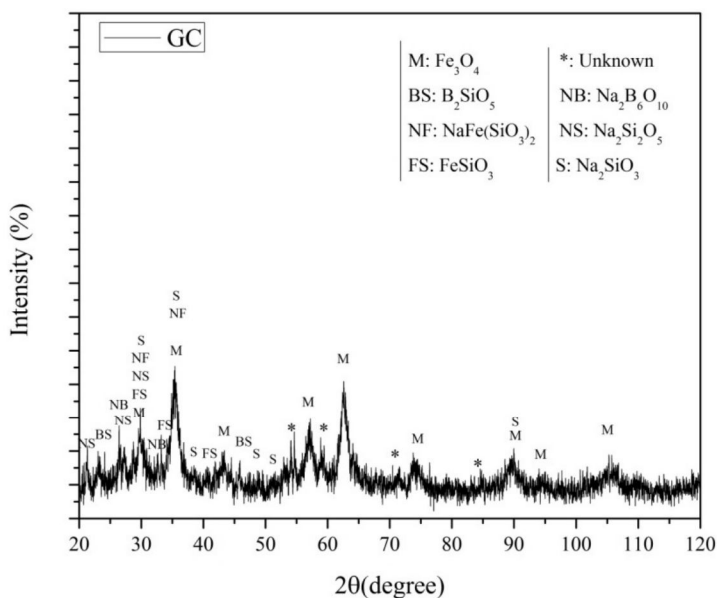


Fig. 2. XRD pattern of glass ceramic (sample GC- 590°C, 1h).

ceramic (sample GC) is  $19.8 \text{ emu g}^{-1}$  and coercive field ( $H_c$ ) is negligible. The value of the maximum  $M_s$  obtained for glass ceramic is different from the theoretically calculated value. If the maximum amount of theoretically feasible magnetite was crystallized in the GC sample, it would have a magnetization value of  $\sim 40 \text{ emu}$

$\text{g}^{-1}$ . This value is obtained by multiplication of the theoretically possible maximum amount of magnetite in this sample GC ( $\sim 43 \text{ wt.}\%$ ) by the magnetite theoretical magnetization value ( $92 \text{ emu g}^{-1}$  [19]).

One of the reasons for this difference could be related to incomplete growth of the magnetite

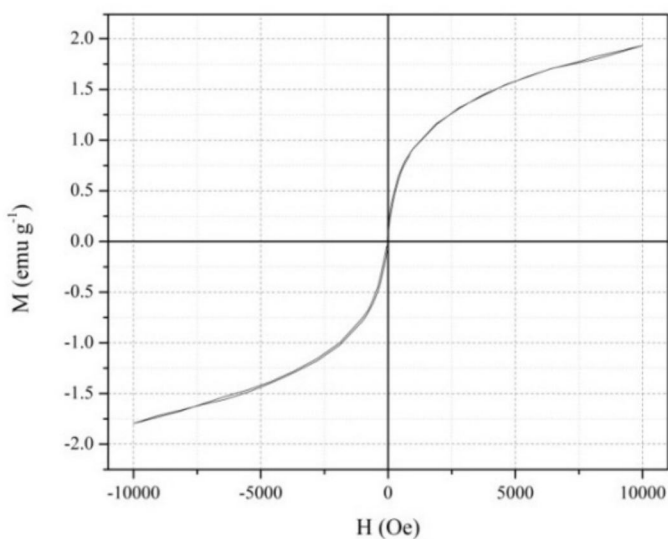


Fig. 3. Hysteresis loop of sample glass.

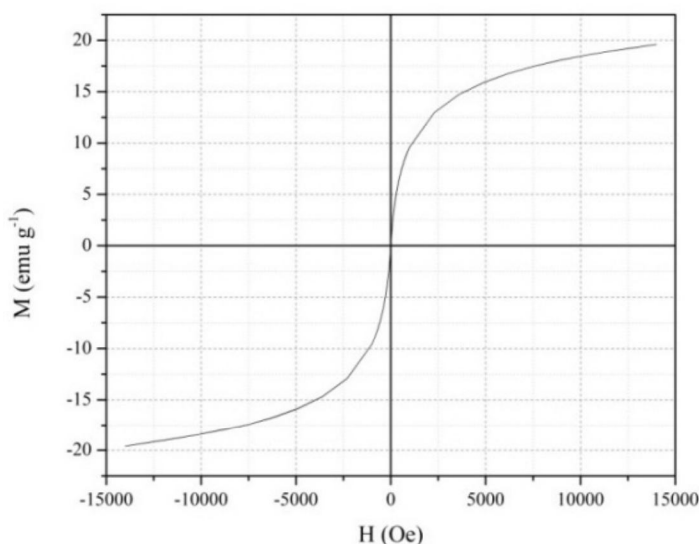


Fig. 4. Hysteresis loop of sample GC.

crystals and their small crystallite size. The saturation magnetization of the magnetite nanoparticles with particle sizes about 7-13 nm have been reported in the range of 52 – 75 emu g<sup>-1</sup> [20].

As observed in the X-ray diffraction pattern of glass ceramic, FeSiO<sub>3</sub> and NaFe(SiO<sub>3</sub>)<sub>2</sub> iron silicate phases were formed during the heat treatment. These phases are non-magnetic and by consuming some of the iron cations in the glass, it would be feasible to decrease the amount of crystallized magnetite phase. Therefore the saturation magnetization would be decreased in the glass ceramic.

### 3. 2. Reduction of Glass and Glass Ceramic

Fig. 5 shows the glass flakes heat treated at 400 °C for 2 h in hydrogen atmosphere (sample GR-400-2). The peaks corresponding to magnetite was observable in the X-ray diffraction pattern. These relatively broad peaks represent of the existence of a fine crystallite size of this phase. Also, from the high background in the X-ray diffraction pattern of the sample could be understood that the amount of crystallized phase in this sample would be very low. The characteristic peak of α-Fe in the X-ray diffraction pattern wasn't observed, so the

reduction of glass in 400 °C for 2 h didn't lead to the formation of α-Fe phase. The reason could be the low permeability and diffusivity of hydrogen in glass at the reduction temperature.

Fig. 6 shows the XRD pattern of the glass flakes heat treated at 590 °C for 1 h in hydrogen

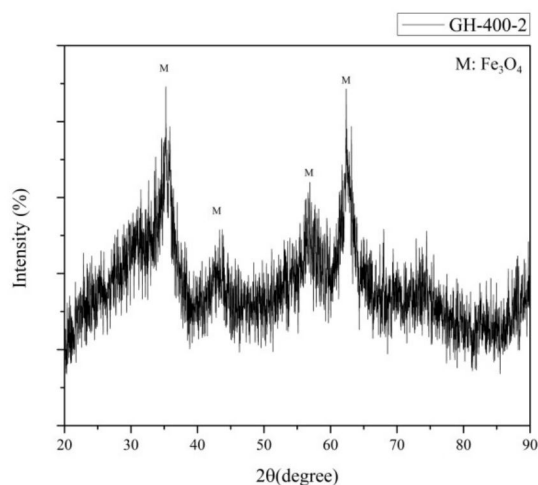


Fig. 5. XRD pattern of GR-400-2 (400 °C, 2 h, H<sub>2</sub> atmosphere).

atmosphere (Sample GR-590-1). It can be seen that by increasing the heat treatment temperature, the  $\alpha$ -Fe and wustite phases have been crystallized with magnetite phase in  $H_2$  atmosphere. The existence of iron phase shows the reduction of iron cations to metallic iron. The hydrogen gas was individually applied in order to reduce glass and the heat treatment temperature was much higher than the  $T_g$  of the glass (373 K) [18]. As a result, the high amount of hydrogen permeability and solubility in glass was expected. It is reported that the reduction mechanism of cations in glass is controlled by the permeability of hydrogen in high hydrogen partial pressure (over 10%) atmosphere and at heat treatment temperatures higher than  $T_g$  of glass [21]. Iron cations could have been reduced in two ways. First, magnetite phase was crystallized in glass and then it reduced to  $\alpha$ -Fe. In the other way, the overall reduction process could be the result of hydrogen diffusion to the site of the iron ions, reduction of the iron ions to the atomic state, diffusion of these atoms to a nuclei, and subsequent growth of these nuclei to form particles of  $\alpha$ -Fe [22].

treated in  $H_2$  atmosphere could be due to the reduction of  $Fe^{3+}$  to  $Fe^{2+}$  cations. Also it has been reported that at temperatures higher than 570 °C, the reduction of magnetite proceeds through the formation of non-stoichiometric wustite [23]. It seems that crystallized magnetite phase reduced during heat-treatment in hydrogen atmosphere and the existence of wustite was probably due to the incomplete reduction of the magnetite phase for 1 hour.

In comparison with sample GR-590-1, in sample GR-675-2, the time and the temperature of the heat treatment in hydrogen atmosphere was increased in order to enhance the hydrogen permeability in glass which would result in reduction of magnetite to the  $\alpha$ -Fe phase.

Fig. 7 shows X-ray diffraction pattern of glass flakes reduced in hydrogen atmosphere for 2 h at 675 °C (GR-675-2). Crystallized phases in the sample GR-675-2 are observed in Fig 7. Besides peaks of  $\alpha$ -Fe phase, the peaks corresponding to the magnetite ( $Fe_3O_4$ ) and wustite ( $FeO$ ) phases were detectable. In this sample, magnetite phase has not been completely transformed to  $\alpha$ -Fe.

Before reduction of the sample GR-590-2-675-

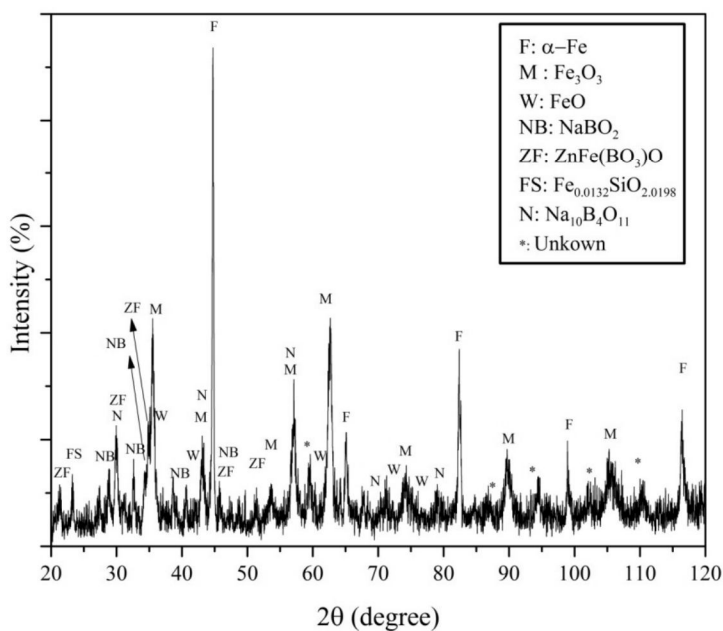


Fig. 6. XRD pattern of GR-590-1 (590 °C, 1 h,  $H_2$  atmosphere).

The existence of wustite in the glass heat 2, it was maintained at 590 °C for 2h in argon

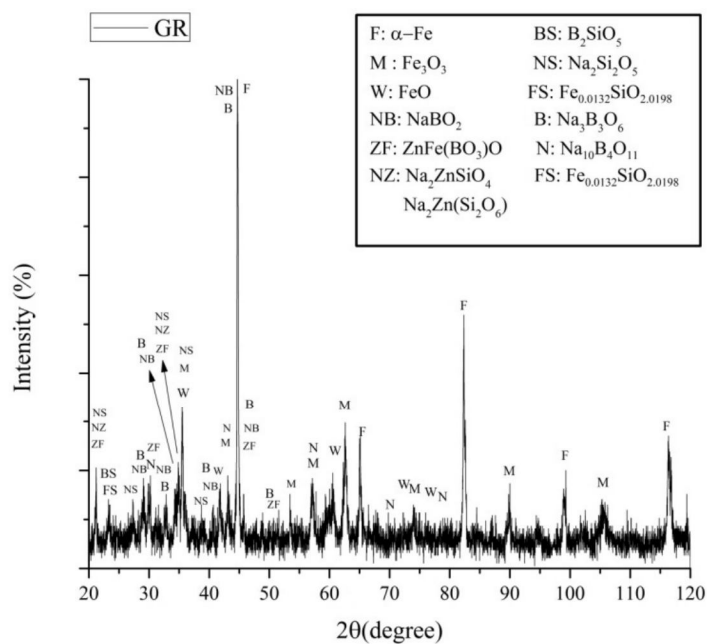


Fig. 7. XRD pattern of GR-675-2 (heat treated at 675 °C for 2 h in H<sub>2</sub> atmosphere).

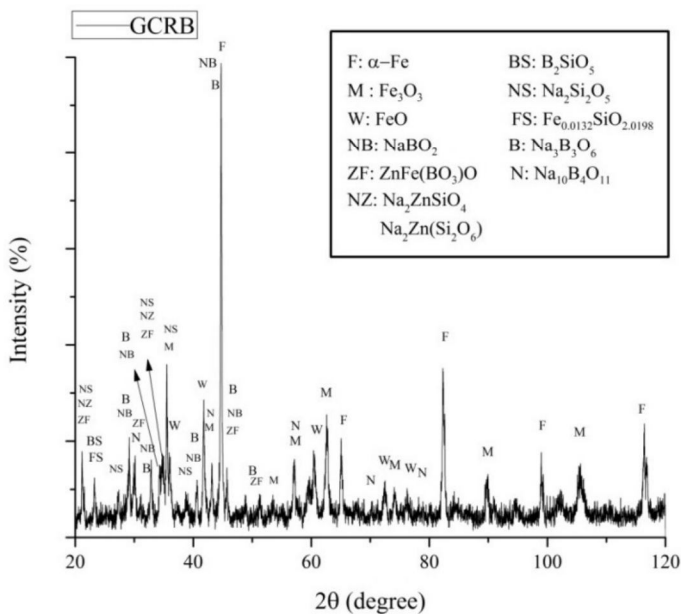


Fig. 8. XRD pattern of GR-590-2-675-2 (heat treated at 590 °C for 1 h in Ar atmosphere and at 675 °C for 2 h in H<sub>2</sub> atmosphere).

atmosphere for crystallization of the magnetite phase in glass. The crystallization and the reduction magnetite were carried out consecutively. XRD pattern of the sample GR-590-2-675-2 is shown in Fig. 8. As seen in this sample, the proportion of FeO peaks intensity to those of  $\alpha$ -Fe increased compared to sample GR-675-2. Because FeO is an intermediate phase of reduction of magnetite to metallic iron, it was likely that the reduction process of magnetite was incomplete.

The powder of sample GC ( $<53 \mu\text{m}$ ) was heat treated at  $675 \text{ }^\circ\text{C}$  for 1 h in hydrogen atmosphere (GCR-675-2). Fig. 9 depicts the XRD pattern of the sample GCR-675-2. It is understood that in comparison to sample GC, The peaks of the magnetite were removed and the characteristic peaks of iron ( $\alpha$ -Fe) were observed. Also iron containing silicate phases in the sample GC such as  $\text{FeSiO}_3$  and  $\text{NaFe}(\text{SiO}_3)_2$  were not detected in the XRD pattern of the sample GCR-675-1. This could be due to the reduction of the iron cations to  $\alpha$ -Fe in these phases.

According to the magnetization results (Fig. 10 and 11) the sample GR-400-2 containing

a maximum magnetization value of  $8 \text{ emu g}^{-1}$  and a very weak coercive force (which could not be measured). In this case, the magnetization never reaches the saturation level and there is no hysteresis loop as a result of presumably the small size of the magnetite particles, falling into the superparamagnetic range. In sample GR-590-1, the magnetization curve approached the saturation level and showed the  $M_s$  value of  $27 \text{ emu g}^{-1}$ . In this case the  $H_c$  value is  $123 \text{ Oe}$ . The  $M_s$  of GR-590-1 was measured higher than GC-590-1. This increase in  $M_s$  can be mainly attributed to the reduction of the magnetite to  $\alpha$ -Fe phase with higher value of  $M_s$  than magnetite ( $\alpha$ -Fe  $M_s=218 \text{ emu g}^{-1}$ ).  $M_s$  and  $H_c$  of sample GR-675-2 was estimated  $37 \text{ emu g}^{-1}$  and  $93 \text{ Oe}$  respectively. By increasing time and temperature of the heat treatment in the sample GR-675-2 in comparison to the sample GR-590-1 probably the amount of the hydrogen permeability in glass increased and higher amount of cations has been reduced.

Hysteresis loop of a two-step reduced glass is given in Fig. 11. The saturation magnetization of this sample was measured  $27 \text{ emu g}^{-1}$  and  $H_c$  was

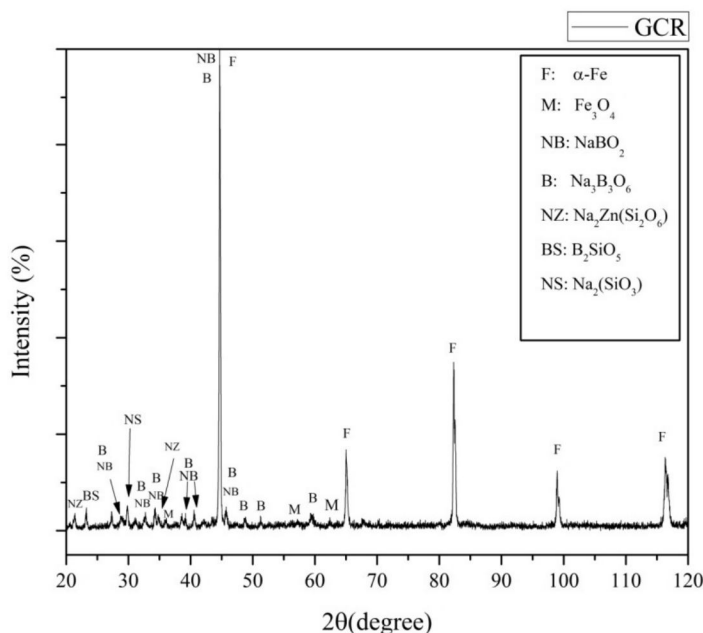


Fig. 9. XRD pattern of GCR-675-1 (glass ceramic heat treated at  $675 \text{ }^\circ\text{C}$  for 1 h in  $\text{H}_2$  atmosphere).

magnetite as the sole crystalline phase, indicates about  $103 \text{ Oe}$ . As observed, with the heat

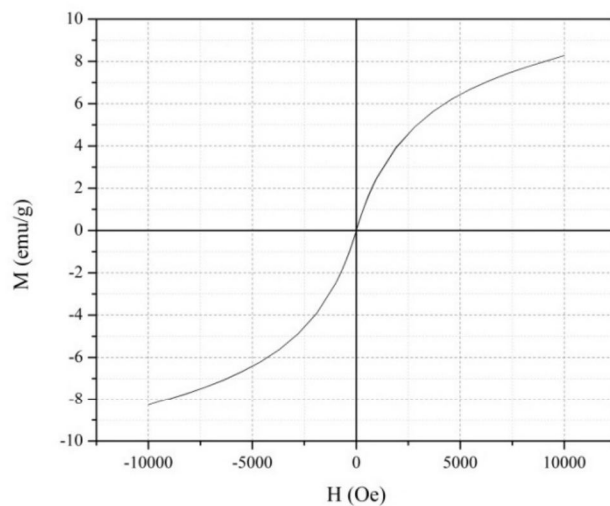


Fig. 10. Hysteresis loop of GR-400-2 (400°C, 2 h).

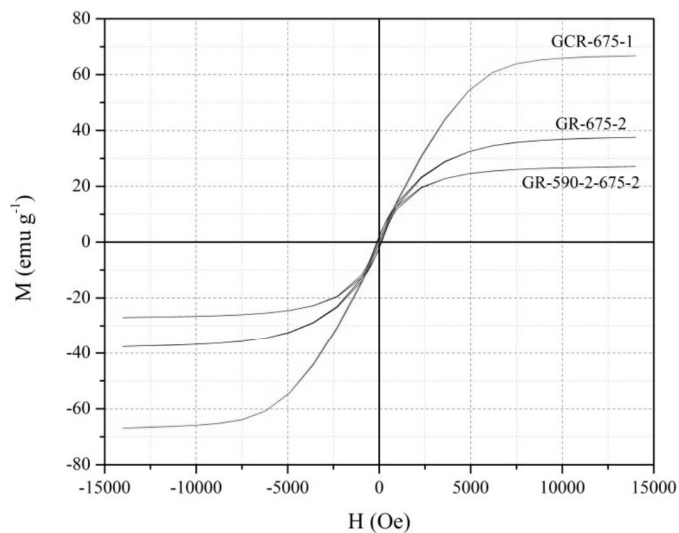


Fig. 11. Hysteresis loop of GCR-675-1, GR-675-2, GR-590-2-675-2.

treatment of the glass at crystallization temperature before the reduction, the saturation magnetization was reduced, presumably due to the incomplete reduction of magnetite and the increase in the FeO amount in the sample. Also some of the iron cations in glass consumed by some non-magnetic silicate phases which leads to

the reduction of the overall magnetization. Direct reduction of glass flakes was unable to reduce all iron cations to metallic iron.

Hysteresis loop of reduced GC powder (GCR-675-1) is shown in Fig. 11. In this sample the magnetization was increased to 67 emu g<sup>-1</sup> which was about three times higher than that of GC. The



value of the maximum  $M_s$  obtained for GCR-675-1 is close to theoretically calculated value. If the maximum amount of theoretically feasible  $\alpha$ -Fe was formed in the GCR-675-1 sample, it should have a magnetization value of  $\sim 77$  emu  $g^{-1}$ . This value is calculated by multiplication of the theoretically feasible maximum amount of  $\alpha$ -Fe in this sample GCR-675-1 ( $\sim 36$  wt.%) by the theoretical magnetization value of  $\alpha$ -Fe ( $218$  emu  $g^{-1}$ ). The difference between  $M_s$  of sample GCR-675-1 and the calculated ones could be induced by changes in the composition during the heat treatment.

The ability of the formation of ferromagnetic phases in glass was observable. Saturation magnetization of ferromagnetic materials is higher than that of ferrimagnetics. Therefore, compared with glass ceramics, the total saturation magnetization of reduced glass ceramics was enhanced.

In the novel magnetic composite materials, obtaining various magnetic properties by changing in the ratio of magnetic phase, the microstructure and composition of ferromagnetic and glass phases might be possible.

#### 4. CONCLUSION

By the use of the rapid roller quenching technique, glass flakes in the  $Na_2O$ - $Fe_2O_3$ - $B_2O_3$ - $SiO_2$ - $ZnO$  system were obtained. Heat treatment of the obtained glass at  $590$  °C for 1 h resulted in the crystallization of magnetite phase and the  $M_s$  value of  $19.8$  emu  $g^{-1}$ . Reduction of glass flakes at  $590$  °C for 1 h and  $675$  °C for 2 h led to the formation of the  $\alpha$ -Fe phase with magnetite and wustite, which exhibited magnetization values of  $27$  and  $37$  emu  $g^{-1}$ , respectively. Reduction of almost all magnetite to  $\alpha$ -Fe phase was observed in reduced glass ceramics containing magnetite phase in a hydrogen atmosphere at  $675$  °C for 1 h.  $M_s$  of this sample increased to  $67$  emu  $g^{-1}$  which was three times higher than that of magnetic ceramic ( $19.8$  emu  $g^{-1}$ ). It seems that a new generation of glass/ferromagnetic composites can be achieved by the reduction of glass ceramics containing ferromagnetic metal compounds.

#### REFERENCES

1. Bayramli, E., Golgelioglu, O. and Ertan, H. B., "Powder metal development for electrical motor applications", *J. Mater. Process. Tech.*, 2005, 16, 83–88.
2. Gimenez, S., Lauwagie, T., Roebben, G., Heylen, W. and Van der Biest, O., "Effects of microstructural heterogeneity on the mechanical properties of pressed soft magnetic composite bodies", *J. Alloys and Comp.*, 2006, 419, 299–305.
3. Shokrollahi, H. and Janghorban, K., "Soft magnetic composite materials (SMCs)", *J. Mater. Process. Tech.*, 2007, 189, 1–12.
4. Yoshizawa, Y., Oguma, S. and Yamauchi, K., "New Fe-based soft magnetic alloys composed of ultrafine grain structure", *J. Appl. Phys.*, 1988, 64, 6044–6047.
5. Anhalt, M., "Systematic investigation of particle size dependence of magnetic properties in soft magnetic composites", *J. Magn. and Magn. Mater.*, 2008, 320, 366–369.
6. Hemmati, H. R., Madaah Hosseini, H. and Kianvash, A., "The correlations between processing parameters and magnetic properties of an iron-resin soft magnetic composite", *J. Magn. and Magn. Mater.*, 2006, 305, 147–151.
7. Akther Hossain, A. K. M., Mahmud, S. T., Seki, M., Kawai, T. and Tabata, H., "Structural, electrical transport, and magnetic properties of  $Ni_{1-x}Zn_xFe_2O_4$ ", *J. Magn. and Magn. Mater.*, 2007, 312, 210–219.
8. Narasimhan, K. S. and Marucci, M. L., "Advances, Applications, and Opportunities for Coated Iron Powder for Electromagnetic Applications", *Magnetic Materials*, in: *Proceedings of the Conference, Euro PM, 2003*, 207–212.
9. Knop, A. and Scheib, W., "Chemistry and Application of Phenolic Resins", Springer, New York, 1979.
10. Zaks, Y., Lo, J., Raucher, D. and Pearce, E. M., "Some structure-properties relationships in polymer flammability: studies of phenolic derived polymers", *J. Appl. Polym. Sci.*, 1982, 27, 913–930.
11. Taghvaei, A. H., Shokrollahi, H. and Janghorban, K., "Magnetic and structural

- properties of iron phosphate- phenolic soft magnetic composites”, *J. Magn. and Magn. Mater.*, 2009, 321, 3926–3932.
12. Taghvaei, A. H., Ebrahimi, A., Ghaffari, M. and Janghorban, K., “Magnetic properties of iron-based soft magnetic composites”, *J. Magn. and Magn. Mater.*, 2010, 322, 808–813.
  13. Tang, G. D., Hou, D. L., Zhang, M., Liu, L. H., Yang, L. X., Pan, C. F., Nie, X. F. and Luo, H. L., “Influence of preparing condition on magnetic properties of the FeCoNi–SiO<sub>2</sub> granular alloy solids”, *J. Magn. and Magn. Mater.*, 2002, 25, 42-49.
  14. Niznansky, D., Viart, N. and Rehspringer, J. L., “Nanocomposites Fe<sub>2</sub>O<sub>3</sub>/SiO<sub>2</sub> -preparation by sol-gel method and physical properties”, *J. Sol-Gel Sci. and Tech.*, 1997, 8, 615-618.
  15. Shull, R. D. and Bennett, L. H., “Nanocomposite magnetic materials”, *J. Nanostructured Mater.*, 1992, 1, 83-87.
  16. Giri, A. K., De Julian, C. and Gonzalez, J. M., “Coercivity of Fe-SiO<sub>2</sub> nanocomposite materials prepared by ball milling”, *J. Appl. Phys.*, 1994, 76, 6573–6575.
  17. Chang, S., Liu, L. and Asher, S. A., “Preparation and properties of tailored morphology, monodisperse colloidal silica-cadmium sulfide nanocomposites”, *J. Am. Chem. Soc.*, 1994, 116, 6739-6747.
  18. Amirahmadi, Z. V. K., Marghussian, A., Beitollahi, Mirkazemi, S. M. and Sarpoolaky, H., “Magnetite nanoparticles prepared by the crystallization of Na<sub>2</sub>O–Fe<sub>2</sub>O<sub>3</sub>–B<sub>2</sub>O<sub>3</sub>–SiO<sub>2</sub> glasses”, *J. Non-Cryst. Sol.*, 2011, 357, 3195–3199.
  19. Codey, J. M. D., “Magnetism and Magnetic Materials”, Cambridge University Press, New York, 2010.
  20. Mascolo, M. C., Pei, Y. and Ring, T. A., “Room Temperature Co-Precipitation Synthesis of Magnetite Nanoparticles in a Large pH Window with Different Bases”, *J. Mater.* 6, 2013, 5549-5567.
  21. Smedskjær, Morten Mattrup, “Structural and Topological Basis of Glass Properties and Diffusion”, PhD thesis, Department of Chemical and Environmental Engineering, Aalborg university, Denmark, 2011.
  22. Tuzzolo, M., R. and Shelby, J. E., “Hydrogen-induced Formation of Colloids of Arsenic, Antimony, and Bismuth in Oxide Glasses”, *J. Non-Cryst. Sol.*, 1992, 143, 181-190.
  23. Pineau, A., Kanari, N. and Gaballah, I., “Kinetics of reduction of iron oxides by H<sub>2</sub>Part II. Low temperature reduction of magnetite”, *Thermochimica Acta*, 2007, 456, 75–88.